RESEARCH REPORTS
Biomaterials & Bioengineering

S.-B. Hong[1], N. Eliaz[2], G.G. Leisk[2], E.M. Sachs[3], R.M. Latanision[2], and S.M. Allen[4]

[1]Harvard School of Dental Medicine, Boston, MA, and Department of Materials Science and Engineering, Massachusetts Institute of Technology, Cambridge, MA; [2]H.H. Uhlig Corrosion Laboratory, Massachusetts Institute of Technology, Cambridge, MA; [3]Department of Mechanical Engineering, Massachusetts Institute of Technology, Cambridge, MA; and [4]corresponding author, Department of Materials Science and Engineering, Massachusetts Institute of Technology, 77 Massachusetts Avenue, Room 13-5018, Cambridge, MA 02139-4307, smallen@mit.edu

J Dent Res 80(3): 860-863, 2001

A New Ti-5Ag Alloy for Customized Prostheses by Three-dimensional Printing (3DP™)

ABSTRACT

Three important considerations in the fabrication of customized cranio-maxillofacial prostheses are geometric precision, material strength, and biocompatibility. Three-dimensional printing (3DP™) is a rapid part-fabrication process that can produce complex parts with high precision. The aim of this study was to design, synthesize by 3DP™, and characterize a new Ti-5Ag (wt%) alloy. Silver nitrate was found to be an appropriate inorganic binder for the Ti powder-based skeleton, and the optimum sintering parameters for full densification were determined. The hardness of the Ti-5Ag alloy was shown to be much higher than that of a pure titanium sample. Potentiodynamic measurements, carried out in saline solution at body temperature, showed that the Ti-5Ag alloy had good passivation behavior, similar to that of pure titanium. It is concluded that the Ti-Ag system may be suitable for fabrication of customized prostheses by 3DP™.

KEY WORDS: prostheses, three-dimensional printing (3DP™), Ti-based alloys, corrosion.

Received July 20, 2000; Last revision January 26, 2001; Accepted February 5, 2001

INTRODUCTION

This study investigated the potential for 3DP™ fabrication of customized complex cranio-maxillofacial prostheses with the use of a new titanium-based alloy. Currently, anatomical reconstruction for the treatment of extensive and complex anatomic bony defects in the cranio-maxillofacial structure involves either autogenous bone graft or implantation of artificial prosthetics made from various biomaterials (*i.e.*, alloplastic implants). While autogenous bone grafts provide tissue compatibility, autograft availability is limited for large defects, and secondary surgery, bone resorption, and donor site morbidity are concerns (Binder and Kaye, 1994). Consequently, alloplastic implants have become an integral part of craniofacial reconstruction.

Titanium is widely used for cranioplasty and oral/maxillofacial repair (Toth *et al.*, 1988; Chandler *et al.*, 1994). It possesses low density, good mechanical properties (*e.g.*, high modulus of elasticity, toughness, and fatigue strength), and biological and chemical inertness. In addition, because of favorable thermal and magnetic properties, titanium is compatible with magnetic resonance imaging (MRI) and computed tomography (CT) scanning. The oxide layer on the surface of titanium and its alloys provides corrosion resistance and allows for histological osseointegration (Sullivan *et al.*, 1994). However, because osseointegration of titanium implants takes a long time (typically from 3 to 6 months), they are often coated with hydroxyapatite [HA, $Ca_{10}(PO_4)_6(OH)_2$]. This bioactive ceramic is more osteoconductive than the titanium surface and can form direct bonds with adjacent hard tissues, leading to an earlier fixation of the implant. Yet, the long-term survivability of HA-coated implants is still controversial, since some clinical reports have indicated failures caused by coating resorption or fatigue.

Three-dimensional printing (3DP™) is a process for the rapid fabrication of three-dimensional parts directly from computer models (Sachs *et al.*, 1992a,b, 1993). An accurate three-dimensional computer model of a customized prosthesis can be designed with the use of a set of CT slices (Fig. 1). This Fig. shows the skull of a patient (13 yrs 7 mos old at the time of scanning) exhibiting congenital multiple defects. Although titanium hardware may not be appropriate for a growing skull, the Fig. clearly demonstrates the potential of 3DP™ for the fabrication of customized cranio-maxillofacial prostheses. The prosthesis model is digitally sliced into discrete cross-sections for 3DP™. The 3DP™ process starts by the spreading of a thin layer of powdered material, which is followed by selective joining of the powder by the printing of a binder material in areas delineated by the model cross-sections. As this process is repeated layer by layer, unbound powder provides temporary support for part overhangs, undercuts, or internal volumes. This unbound powder is removed upon process completion, leaving the finished "green" (packed) part.

Several significant advantages of 3DP™ over other processes in customized prosthesis fabrication include: an ability to produce complex geometry and small dimensions with high precision (*e.g.*, feature-size resolution on the order of 100 microns, which is not attainable in casting or

milling of titanium); a potential for scaling-up in size and rate with multiple printheads; and adaptability to different material systems, including ceramics and functionally graded materials (FGMs). Unfortunately, suitable material systems that exhibit the vital combination of strength and biocompatibility for prosthetic applications have yet to be identified. Thus, the objective of this work was to design and synthesize by 3DP™ a new titanium-based alloy, followed by study of its suitability for fabrication of customized prostheses (through hardness testing, electrochemical measurements, and surface analysis).

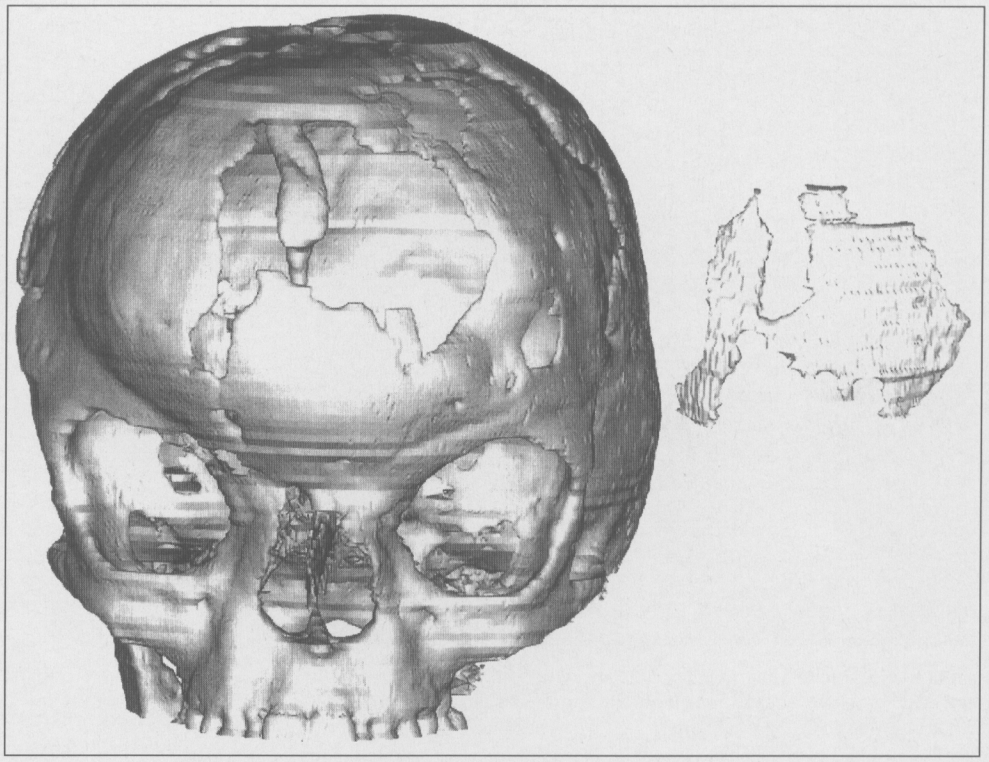

Figure 1. Computer model of skull exhibiting congenital multiple defects made from CT scans sliced at 1-mm intervals (left), and computer reconstruction of the defects (right).

MATERIALS & METHODS

Titanium Powder

Due to its good sinterability and flowability, a spherical atomized pure titanium powder was selected for this work. The commercial powder (99.9% pure, Surepure Chemetals, Florham Park, NJ, USA) size was 60 ± 15 μm in diameter. A scanning electron microscope, SEM (XL30 ESEM-FEG, Philips, Eindhoven, The Netherlands), was used to characterize the shapes of the powder particles and their surface smoothness. X-ray diffraction, XRD (Rotaflex, Rigaku, Osaka, Japan), was used to determine the crystallographic structure of the powder particles at room temperature. The flowability of the powder was estimated through measurement of its angle of repose (ASTM, 2000).

Three-dimensional Printing (3DP™)

Binders are used in 3DP™ to join the powder particles selectively during printing (Guo, 1998). Four different wax- and acrylic-polymer-based binders were shown to introduce carbon contamination into the final sintered part (Hong, 2000). To avoid this problem, inorganic reactive binders were selected for use. Because silver exhibits high solubility and diffusivity in titanium, 2 silver salts were examined as potential binders. However, since silver carbonate (Ag_2CO_3) was shown to provide unsatisfactory binding of the titanium particles (Hong, 2000), only silver nitrate ($AgNO_3$) has been used in this work. A 5.8-M aqueous solution of $AgNO_3$ (Alfa Aesar, Ward Hill, MA, USA) was deposited as droplets into a titanium powder bed. The powder bed was subsequently heated for 1 hr at 450°C under argon gas atmosphere in an alumina tube furnace. Because the initial sintering temperature (*i.e.*, the minimum temperature at which the powder starts to sinter but still easily disintegrates due to weak binding), T_s, of titanium powders is higher than 500°C (Hong, 2000), unbound powders were eventually removed easily from the surface of the bound part after treatment at 450°C. The microstructure of the sintered part was characterized by SEM and XRD. We evaluated the mechanical integrity of the sintered parts by placing them in an ultrasonic bath (GT-120, LECO, St. Joseph, MI, USA) for a few minutes.

Sintering

Full densification of the printed samples was achieved in a final sintering stage. Since titanium powders are typically sintered to full density under vacuum at a temperature higher than 1100°C, the Ti-Ag system involves liquid-phase sintering to full densification. Therefore, both minimum porosity and uniform shrinkage should be ensured—the former for improved mechanical properties and passivation behavior, and the latter for dimensional stability. The shrinkage resulting from silver reduction was found to be negligible in comparison with the overall shrinkage during full densification (Hong, 2000). A set of experiments was designed to evaluate the effects of both temperature and heating rate on the material porosity. We measured the number of pores and their sizes by analyzing SEM micrographs of sintered samples with an image analysis software package (NIH Image 1.62, NIH, Bethesda, MD, USA), following a standard procedure (ASTM, 1999). The pore size was found to be lognormally distributed. The porosity (*i.e.*, the volume fraction of pores) was found to increase with increasing heating rate and decreasing sintering temperature (Hong, 2000).

Characterization Techniques

The fully sintered samples were characterized by means of microhardness testing, electrochemical measurements, and surface analysis. For comparison, the same experiments were carried out on pure titanium control samples. These samples were cut from a 3.175-mm-thick plate (Alfa Aesar, Ward Hill, MA, USA), formed by a sequence of hot rolling, cold rolling, and annealing operations. Microhardness measurements (DM-400, LECO, St. Joseph, MI, USA) were conducted with a Vickers indenter at a load of 200 g and loading duration of 15 sec. Electrochemical measurements were carried out on specimens

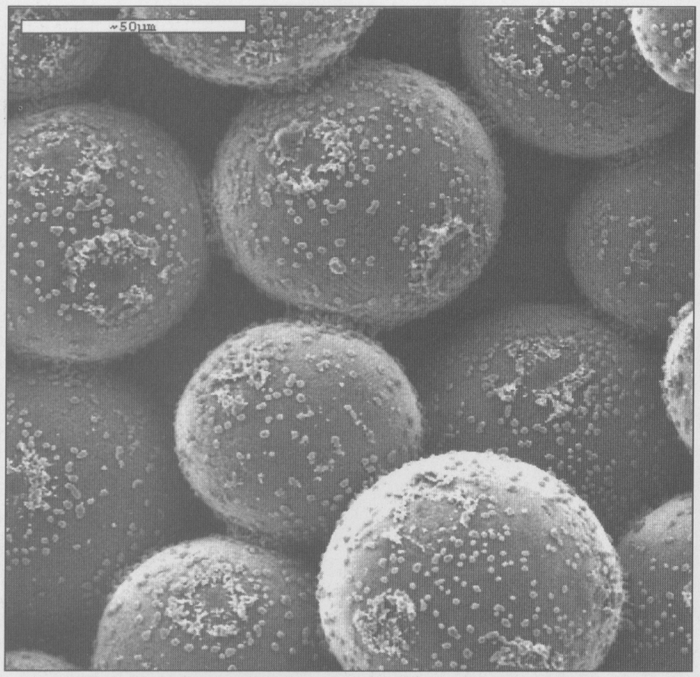

Figure 2. Typical SEM micrograph showing the binding of titanium particles by silver necks following sintering of the titanium powder and silver nitrate binder at 450°C.

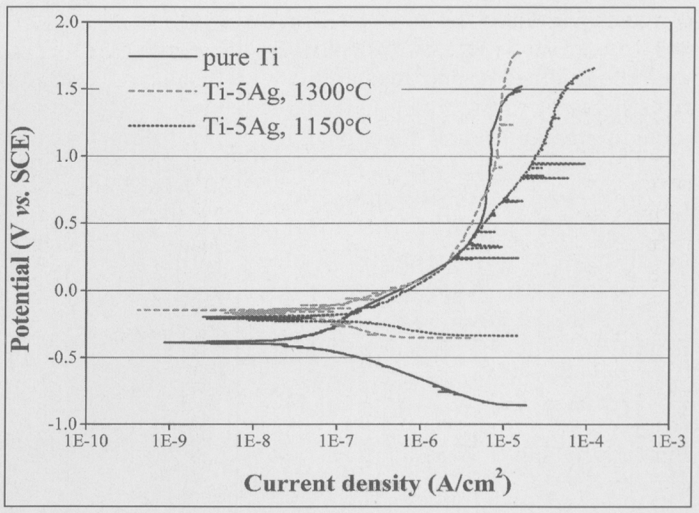

Figure 3. Typical potentiodynamic curves for Ti-5Ag (wt%) alloy made by 3DP™ and sintered at either 1300 or 1150°C. The equivalent curve for the pure titanium control sample is shown for comparison. The Ti-5Ag alloy sintered at 1300°C exhibits the lowest corrosion current density and the most noble corrosion potential.

with an exposed area of approximately 1 x 1 cm^2. We carried out both rest potential measurements and potentiodynamic measurements on 4 specimens to ensure repeatability. Each specimen was prepared in three steps: First, a copper wire was attached to the sample by both a silver paint (Ernest F. Fullam, Latham, NY, USA) and 5 Minute® Epoxy (ITWDevcon, Danvers, MA, USA). A glass tube was epoxied to the sample to prevent exposure of the wire to the electrolyte. Next, the sample was mounted in an Epo-Thin® cold-mount resin (Buehler, Lake Bluff, IL, USA). Finally, after being cured, the specimen was ground with 600-grit grinding paper. A standard three-electrode system (Jones, 1996) was used for the electrochemical measurements, with a saturated calomel electrode (SCE) as a reference electrode, and pure platinum foil as a counter-electrode. A non-de-aerated saline solution (0.9% NaCl [Mallinckrodt Baker, Paris, KY, USA], pH 5.5), maintained at body temperature (~37°C), was used as the electrolyte. The rest potential, E_{OC}, was monitored for 20 min by means of an electrochemical interface (Model SI 1286, Schlumberger, Hampshire, England). Subsequently, potentiodynamic measurements were carried out at a scan rate of 1.0 mV/sec from -200 mV *vs.* E_{OC} to +1500 mV *vs.* reference electrode. The corrosion current density, i_{corr}, was determined through extrapolation of the cathodic polarization curve (potentiodynamic measurement).

RESULTS

SEM observations of the as-received titanium powder showed that the particles had both a highly spherical shape and smooth surfaces. XRD experiments confirmed that the particles were of the hexagonal close-packed (hcp) α-Ti phase. The angle of repose measured for the titanium powder was 23.3 ± 1.5 deg.

After the addition of the $AgNO_3$ binder and sintering at 450°C, the silver reduced from $AgNO_3$ formed well-defined necks between the titanium particles, thus binding them together (Fig. 2). XRD indicated the co-existence of α-Ti and Ag in the sintered part. The sintered parts were found to have good mechanical integrity, withstanding vibrations in an ultrasonic bath for more than a few minutes.

The hardness values for the Ti-5Ag alloy after densification at two different temperatures are shown in the Table in comparison with a pure titanium control sample. The printed Ti-5Ag alloy exhibits much higher hardness in comparison with the control sample. Fig. 3 shows typical potentiodynamic curves for the three materials. The shapes of the curves for the control sample and for the Ti-Ag alloy sintered at 1300°C are similar, although the latter exhibits a less active (*i.e.*, less negative) corrosion potential. The alloy sintered at 1150°C exhibits less passivation at high potentials in comparison with the other two materials. All three materials exhibit similar

Table. Experimental Results for New Ti-5Ag (wt%) Alloys Made by Three-dimensional Printing (3DP™), Indicating Increased Hardness and Corrosion Resistance over Pure Titanium (values given as mean ± standard deviation)

Sample	Fabrication	Porosity[a] %	Hardness[b] VHN	E_{corr}[c] mV	i_{corr}[d] A/cm^2
Pure Ti[e]	Rolling and annealing	0	204 ± 7	-380 ± 42	(1.3 ± 0.3) E-7
Ti-5Ag	Sintered at 1300 C[f]	1.50 ± 0.73	700 ± 38	-210 ± 35	(7.8 ± 0.2) E-7
Ti-5Ag	Sintered at 1150 C[f]	6.30 ± 3.30	429 ± 26	-230 ± 31	(8.9 ± 0.5) E-7

[a] Based on image analysis of SEM micrographs with 7 fields in each sample.
[b] Based on 5 microhardness measurements each, in Vickers Hardness Number units.
[c] Rest potential was measured *vs.* saturated calomel reference electrode after 20-minute run (4 measurements each).
[d] Corrosion current density obtained from the potentiodynamic curve generated in first hour of immersion in saline solution (4 measurements each).
[e] Control sample (plate).
[f] Heating rate, 2°C/min

corrosion current density. Typical values of the rest potential and the corrosion current density are shown in the Table.

DISCUSSION

Characterization of the as-received titanium powder provided several promising indications as to its applicability to 3DP™ fabrication. First, the small powder diameter allows for reduction of the minimum thickness of printed layer attainable. The large surface area of such powder should also provide a large driving force for sintering. Second, the smooth surfaces of the particles should enhance powder flowability and, hence, printability. The flowability can also be improved by the presence of a thin oxide layer with higher hardness and lower friction coefficient on the surface of the titanium powder. Finally, the angle of repose measured in this work is smaller than 25 deg, a threshold value above which a smooth powder bed is difficult to achieve (Hong, 2000).

The aqueous solution of silver nitrate was found to be a good binder for prosthetic fabrication by 3DP™. It formed strong interparticle silver necks at temperatures lower than the initial sintering temperature of titanium powders, and did not introduce carbon contamination. The good particle binding provided by this binder may be related to the wide gap between its melting temperature (212°C) and its decomposition temperature to form solid silver (444°C). This binder, however, has a significant drawback that has to be considered. Because of the high corrosiveness of this solution, it causes some irritation to human skin and is destructive to the 3DP™ equipment. Thus, a safe printing procedure has to be established. Since the conventional type of high-speed bubble-jet printhead is not recommended for use with silver nitrate, the use of a piezo-based printhead is currently being studied.

Suitable parameters (temperature, heating rate, and time at maximum temperature) for the final-stage sintering of the Ti-5Ag alloy were determined in this work. The sample that was sintered at 1300°C for 1 hr at a heating rate of 2°C/min exhibited both fairly low porosity (1.50% ± 0.73%) and a narrow distribution of pore size.

The sintered Ti-Ag alloy exhibited high hardness, a desirable property of materials for prosthesis construction. Basic design criteria for surgical prostheses also require that the material be sufficiently inert in the *in vivo* environment. For most metallic biomaterials, including titanium, corrosion resistance is derived from their ability to form surface-passive films and to retain them under the *in vivo* environment. The half-cell electrode potential for hydrogen evolution obtained from the Nernst equation (Jones, 1996) at pH 5.5 is –0.56 V (*vs.* SCE). Because the corrosion potential values measured for all samples were less negative than this value, it may be assumed that oxygen reduction is the major cathodic reaction. It should be noted that because oxygen reduction is more oxidizing than hydrogen evolution in the saline solution, the absence of de-aeration (*e.g.*, by nitrogen gas bubbling) in this work resulted in a relatively corrosive environment. Yet, the Ti-5Ag alloy exhibited a more noble rest potential in comparison with pure Ti, probably due to the higher exchange current density for hydrogen/oxygen reduction on silver than on titanium. The slightly more noble rest potential for the sample sintered at 1300°C in comparison with the one sintered at 1150°C may be attributed to a more even distribution of silver in the former. With regard to corrosion behavior, the Ti-5Ag alloy looks promising. However, it should be noted that corrosion resistance is only a partial indication of biocompatibility. Cell culture and/or animal studies should be carried out before implantation of any prosthesis into human bodies.

ACKNOWLEDGMENTS

This work was supported by the 3DP™ group at MIT and made use of shared facilities at MIT Center for Materials Science and Engineering (CMSE), which is supported by the National Science Foundation under award number DMR-9400334. This work is based on a thesis approved by the Harvard School of Dental Medicine in partial fulfillment of the requirements for the degree of Doctor of Medical Sciences in the subject of Oral Biology. A preliminary report was presented at the 78th General Session & Exhibition of the International Association for Dental Research, held in Washington, DC, April 5–8, 2000.

REFERENCES

ASTM (1999). Standard practice for determining the inclusion or second-phase constituent content of metals by automatic image analysis. ASTM E 1245-95. In: 1999 annual book of ASTM standards. Vol. 03.01. West Conshohocken, PA: American Society for Testing and Materials.

ASTM (2000). Standard test method for flow rate of metal powders. ASTM B 213-97. In: Annual book of ASTM standards 2000. Vol. 02.05. West Conshohocken, PA: American Society for Testing and Materials.

Binder WJ, Kaye A (1994). Reconstruction of post-traumatic and congenital facial deformities with three-dimensional computer-assisted custom-designed implants. *Plast Reconstr Surg* 94:775-787.

Chandler CL, Uttley D, Archer DJ, MacVicar D (1994). Imaging after titanium *cranioplasty*. *Br J Neurosurg* 8:409-414.

Guo H (1998). Alloy design for three-dimensional printing of hardenable tool materials (dissertation). Cambridge, MA: Massachusetts Institute of Technology.

Hong SB (2000). Individualized cranio-maxillo-facial prosthesis construction using three-dimensional printing (3DP™) with atomized titanium powder (dissertation). Boston, MA: Harvard School of Dental Medicine.

Jones DA (1996). Principles and prevention of corrosion. 2nd ed. Upper Saddle River, NJ: Prentice-Hall.

Sachs E, Cima M, Bredt J, Curodeau A (1992a). CAD-casting: the direct fabrication of ceramic shells and cores by three-dimensional printing. *Manuf Rev* 5:118-126.

Sachs E, Cima M, Williams P, Brancazio D, Cornie J (1992b). Three-dimensional printing: rapid tooling and prototypes directly from a CAD model. *J Eng Indust* 114:481-488.

Sachs E, Haggerty J, Williams P, Cima M (1993). Three dimensional printing techniques. US Patent 5,204,055. April 20.

Sullivan PK, Smith JF, Rozzelle AA (1994). Cranio-orbital reconstruction: safety and image quality of metallic implants on CT and MRI scanning. *Plast Reconstr Surg* 94:589-596.

Toth BA, Ellis DS, Stewart WB (1988). Computer-designed prostheses for orbito-cranial reconstruction. *Plast Reconstr Surg* 81:315-324.